Hong Kong J Radiol. 2021;24:219-28 | https://doi.org/10.12809/hkjr2117394

PICTORIAL ESSAY

Differential Diagnoses of Axillary Lesions: a Pictorial Essay

TKB Lai, T Wong, CM Chau, WY Fung, RLS Chan, AWT Yung, JKF Ma

Department of Diagnostic and Interventional Radiology, Princess Margaret Hospital, Hong Kong

INTRODUCTION

Axillary mass or swelling is a common clinical presentation that requires imaging investigation. There is a wide range of differential diagnoses because the axilla contains both lymph nodes and non-lymphatic tissue such as accessory breast tissue, skin, fat, muscles, nerves, blood vessels, and is surrounded by bone. Radiologists should be familiar with the axillary anatomy and imaging features of different axillary lesions.

This pictorial essay provides an imaging review and diagnosis of axillary lesions that arise from different anatomical structures using different imaging modalities including ultrasonography (US), mammography, plain radiography, computed tomography (CT), magnetic resonance imaging (MRI), and angiography.

ANATOMY

A basic understanding of axillary anatomy is essential for both lesion detection and differentiation. The axilla resembles a pyramid.[1,2] There are pectoralis muscles anteriorly, and the scapula, latissimus dorsi and teres major muscles posteriorly.[1] The medial and lateral boundaries comprise the chest wall and proximal humerus, respectively.[1] The base is covered by skin, while the apex, which contains neurovascular structures, is bounded by the first rib, clavicle, and superior scapular border.[1]

LYMPH NODES

Axillary lymph nodes are divided into three levels by the pectoralis minor muscle. Level I is inferolateral to the pectoralis minor; level II behind the pectoralis minor; and level III superomedial to the pectoralis minor. A complete US examination of these lymph nodes should scrutinise the entire fatty content from the margin of the pectoralis muscles to the latissimus dorsi and teres major muscles and should include the axillary tail.[3]

Differentiating malignant lymph nodes from benign is no easy task due to the presence of overlapping features. Changes such as cortical thickening (Figure 1a), hilum loss, or changes in shape or vascular pattern, are considered suspicious.[4]

A benign lymph node has a thin or invisible cortex and a fatty hilum due to connective tissue trabeculae, lymphatic tissue cords, and medullary sinusoids.[4] The cortex is hypoechoic on US, while the hilum is echogenic on US and lucent on mammography. Various cut-off points have been reported for a normal cortical

Correspondence: *Dr TKB Lai, Department of Diagnostic and Interventional Radiology, Princess Margaret Hospital, Hong Kong*
Email: laiterencekb@gmail.com

Submitted: 11 May 2021; Accepted: 15 Jul 2021

Contributors: All authors designed the study and acquired the data. TKBL, TW and CMC analysed the data. TKBL drafted the manuscript. All authors critically revised the manuscript for important intellectual content. All authors had full access to the data, contributed to the study, approved the final version for publication, and take responsibility for its accuracy and integrity.

Conflicts of Interest: All authors have disclosed no conflicts of interest.

Funding/Support: This study received no specific grant from any funding agency in the public, commercial, or not-for-profit sectors.

Data Availability: All data generated or analysed during the present study are available from the corresponding author on reasonable request.

Ethics approval: This study was approved by the KWC Research Ethics Committee (Ref: KW/EX-20-146(153-04)) and conducted in accordance with the Declaration of Helsinki.

Declaration: Part of the material from this study was accepted as an e-poster presentation at the 28th Annual Scientific Meeting of Hong Kong College of Radiologists, 14-15 November 2020.

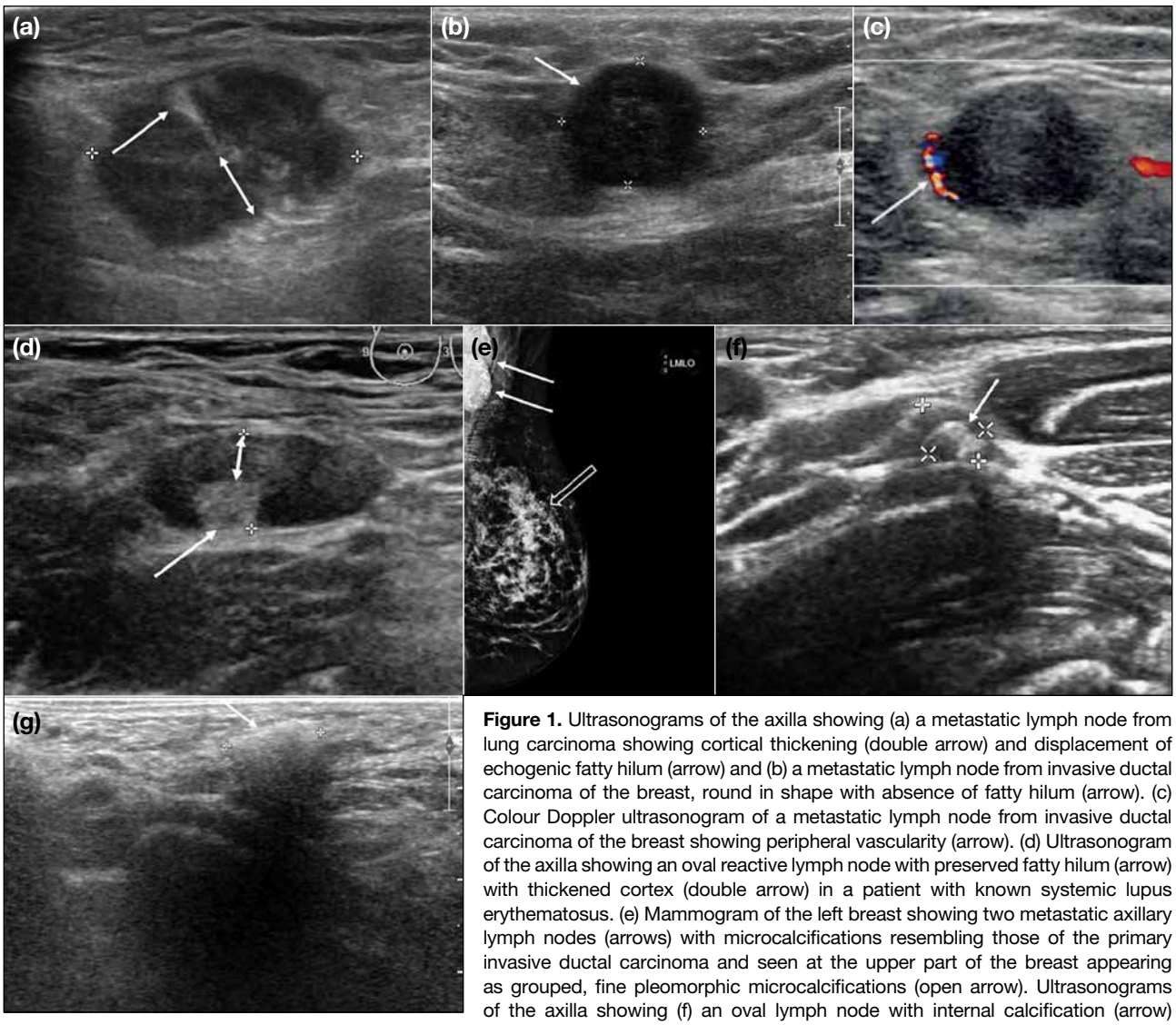

Figure 1. Ultrasonograms of the axilla showing (a) a metastatic lymph node from lung carcinoma showing cortical thickening (double arrow) and displacement of echogenic fatty hilum (arrow) and (b) a metastatic lymph node from invasive ductal carcinoma of the breast, round in shape with absence of fatty hilum (arrow). (c) Colour Doppler ultrasonogram of a metastatic lymph node from invasive ductal carcinoma of the breast showing peripheral vascularity (arrow). (d) Ultrasonogram of the axilla showing an oval reactive lymph node with preserved fatty hilum (arrow) with thickened cortex (double arrow) in a patient with known systemic lupus erythematosus. (e) Mammogram of the left breast showing two metastatic axillary lymph nodes (arrows) with microcalcifications resembling those of the primary invasive ductal carcinoma and seen at the upper part of the breast appearing as grouped, fine pleomorphic microcalcifications (open arrow). Ultrasonograms of the axilla showing (f) an oval lymph node with internal calcification (arrow) causing posterior acoustic shadowing in a child with recent Bacillus Calmette–Guérin (BCG) vaccination, consistent with BCG lymphadenitis and (g) "snowstorm appearance" in an axillary lymph node (arrow) with silicone deposition in a patient who presented with ruptured silicone breast implant (not shown).

thickness, with an upper limit ranging from 2.3 mm to 3 mm.[4] Absence of the hilum is the most specific finding for metastatic disease, but such finding is present only in cases of advanced disease.[4]

A benign lymph node is usually <2 cm in maximal diameter.[3] Nonetheless size criteria are reported to be less essential to identify metastasis.[3] A benign lymph node is normally oval or elliptical in shape. On the contrary, a malignant node is often round (Figure 1b) and has a short to long axes ratio of >0.5.[5]

Nodal vascularity on Doppler US generally follows two patterns: central or peripheral.[4] The central pattern shows a single hilum vascular signal or dispersed signals distributed at the centre of the node and is usually found in the absence of malignancy.[4] The peripheral pattern (Figure 1c) demonstrates a linear signal at the periphery of the node and is more common in lymph nodes with metastases.[4]

Causes of unilateral axillary lymphadenopathy can be benign and include infection such as mastitis[6] and post-vaccination reactions, for example from influenza, human papillomavirus, Bacillus Calmette–Guérin, or coronavirus disease 2019 vaccination.[7] Malignant causes include metastasis from breast malignancy and non-breast malignancies.[6]

Bilateral axillary lymphadenopathy can be due to systemic aetiologies such as wide-spread infection, rheumatoid arthritis, collagen vascular disease such as systemic lupus erythematosus (Figure 1d), lymphoma, leukaemia, and metastatic non-breast tumour.[6]

Calcifications in abnormal axillary lymph nodes may represent calcified metastasis from breast (Figure 1e), thyroid or ovarian cancer, collagen vascular disease, or granulomatous infections such as tuberculosis and Bacillus Calmette–Guérin lymphadenitis (Figure 1f).[3] Migrated silicone from an augmented breast and migrated gold particles in rheumatoid arthritis patients receiving gold therapy can mimic calcifications in lymph nodes, and can usually be differentiated by a relevant clinical history.[6] Silicone deposition in an axillary lymph node is typically hyperechoic with a well-defined anterior margin and a poorly defined posterior margin, giving a characteristic "snowstorm appearance" (Figure 1g).

It should be noted that imaging criteria are not completely reliable in differentiating benign from malignant lymph nodes. For those with suspicious features, image-guided fine needle aspiration cytology or biopsy can offer additional information.

Non-nodal Lesions

Knowledge of a relevant clinical presentation such as prior axillary surgery, breast augmentation or active local infection can help diagnose certain surgery-related non-nodal axillary pathologies.

Surgery-Related Lesions

Post-surgical lesions in the axilla include seromas, haematomas, fat necrosis, and suture granulomas. Seromas (Figure 2a) typically appear as loculated fluid collections close to the operative bed, with or without fluid-debris levels on US and MRI scans.[8]

Haematomas may show variable internal architecture on imaging, depending on the evolution of the blood products (Figure 2b,c).[8] Appearance ranges from being anechoic on US during the hyperacute phase, with progressive development of mixed internal echoes due to formation of blood clots, to finally becoming lesions with irregular walls and internal septations in the subacute to chronic phase.[2]

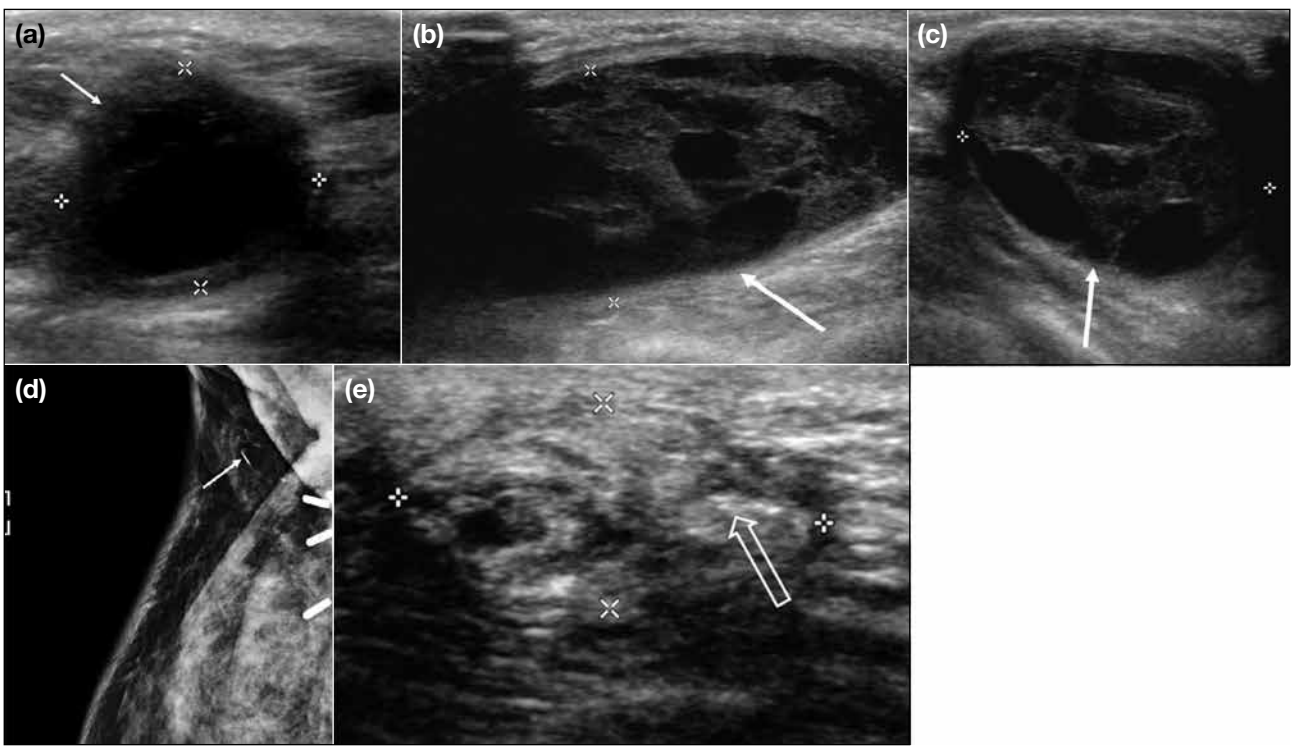

Figure 2. Ultrasonograms of the axilla showing: (a) a well-circumscribed, predominantly anechoic lesion adjacent to a scar, typical of a seroma (arrow); (b) heterogeneous lesions with fluid and non-fluid components in a patient with recent axillary dissection consistent with haematomas (arrow); and (c) interval shrinkage of the haematomas (arrow) in subsequent follow-up imaging. (d) Mammogram of the right breast showing a fat-density lesion with dystrophic calcifications in the axilla (arrow). (e) Ultrasonogram of the right axilla showing a corresponding hyperechoic lesion with internal calcifications (open arrow). Findings are consistent with fat necrosis.

Fat necrosis is a benign inflammatory process resulting from vascular insult to fat cells, and its imaging findings are reported to correspond to the stage of development and maturation.[8] Appearance on mammography ranges from a speculated mass to calcifications (Figure 2d,e). It can appear cystic on US and may contain echogenic bands that are specific for fat necrosis. Features on MRI scans correspond to the extent of inflammation and fibrosis. It often exhibits hypointense signal on T1-weighted sequences and may demonstrate variable enhancement in post-contrast images.[2]

Suture granuloma occurs due to local inflammation in response to retained suture material. It is characterised by a hypoechoic lesion with hyperechoic lines on US that represent the sutures.[8]

All these post-surgical lesions may be difficult to differentiate from malignancy and biopsy is required.[8]

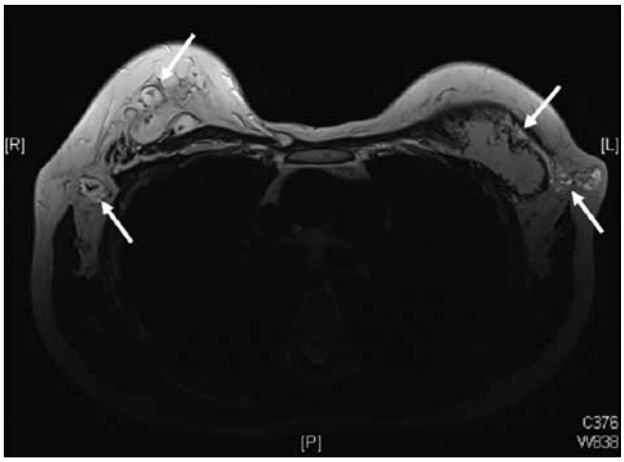

Figure 3. T2-weighted magnetic resonance image showing hyperintense collections in the right breast, left retropectoral region, and both axillae in this patient with history of breast augmentation are consistent with polyacrylamide gel migration (arrows).

Breast Augmentation–Related Lesions

They are mainly related to migration of ruptured implants or injected materials. Examples include silicone deposits in axillary lymph nodes as described previously, and polyacrylamide gel migration to the axilla as a consequence of breast augmentation (Figure 3). Migrated polyacrylamide gel appears as small loculations with MRI signal intensity similar to that of water and can form nodules in the axilla.[9]

Infective or Inflammatory Lesions

This entity includes abscesses.[1] Local injury, sweat or sebaceous gland obstruction, and hair follicle infection can result in abscess formation.[2] Abscesses can also occur within the lymph nodes as a result of bacterial or tuberculosis lymphadenitis.[2] On US, they can appear as a hypoechoic fluid collection with internal debris or loculations and a hypervascular echogenic wall.[2] On contrast cross-sectional imaging, they usually show peripheral rim enhancement (Figure 4).

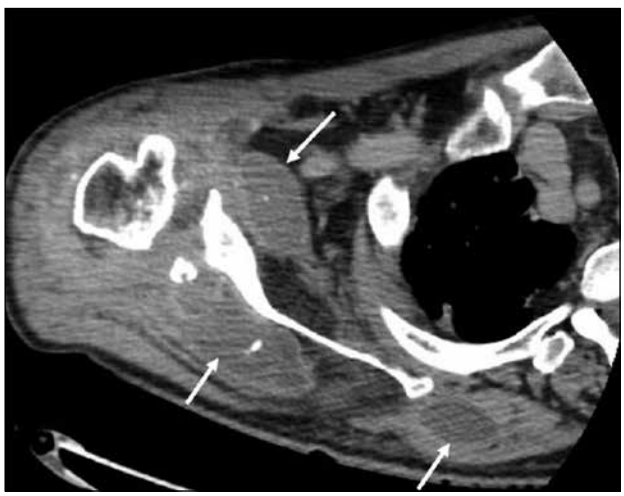

Figure 4. Post-contrast computed tomography image showing multiple rim-enhancing collections, including one in the right axilla with calcification in this patient with known systemic tuberculosis, consistent with abscesses (arrows).

Other non-nodal pathologies can be categorised according to their anatomical origin and managed accordingly.

BREAST TISSUE

Accessory Breast Tissue

This is a normal variant resulting from failed regression of embryonic mammary tissue, most often located in the axilla and is susceptible to the same benign and malignant pathologies that develop in the normal breast.[3] On mammography and US, there is a varying amount of fibroglandular elements among fat that radiologically resembles normal glandular tissue but is separate from the main breast parenchyma (Figure 5).[2,3]

Axillary Tail Lesions

Axillary tail is a continuous extension of the upper outer quadrant breast tissue. Therefore benign lesions such as cyst (Figure 6a,b) can develop in the axillary tail as in the rest of the breast. Breast carcinoma (Figure 6c,d) in the axillary tail is extremely rare.[10]

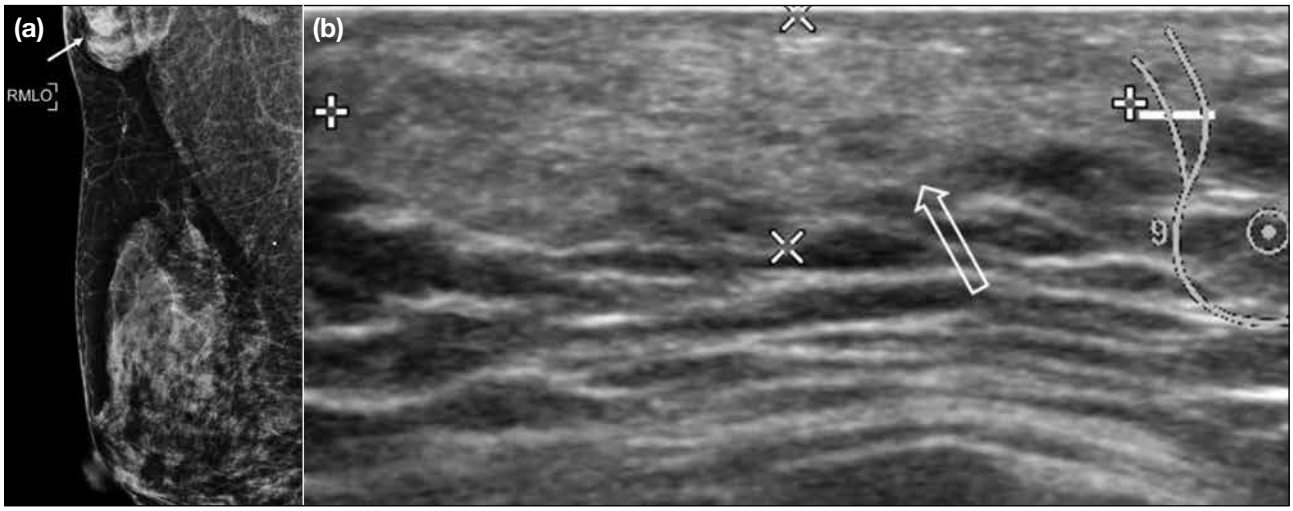

Figure 5. (a) Mammogram and (b) ultrasonogram showing accessory breast tissue in two different patients, appearing as a varying amount of fibroglandular elements interspersed with fat that resemble the appearance of normal glandular tissue but are located in the axilla (arrow and open arrow).

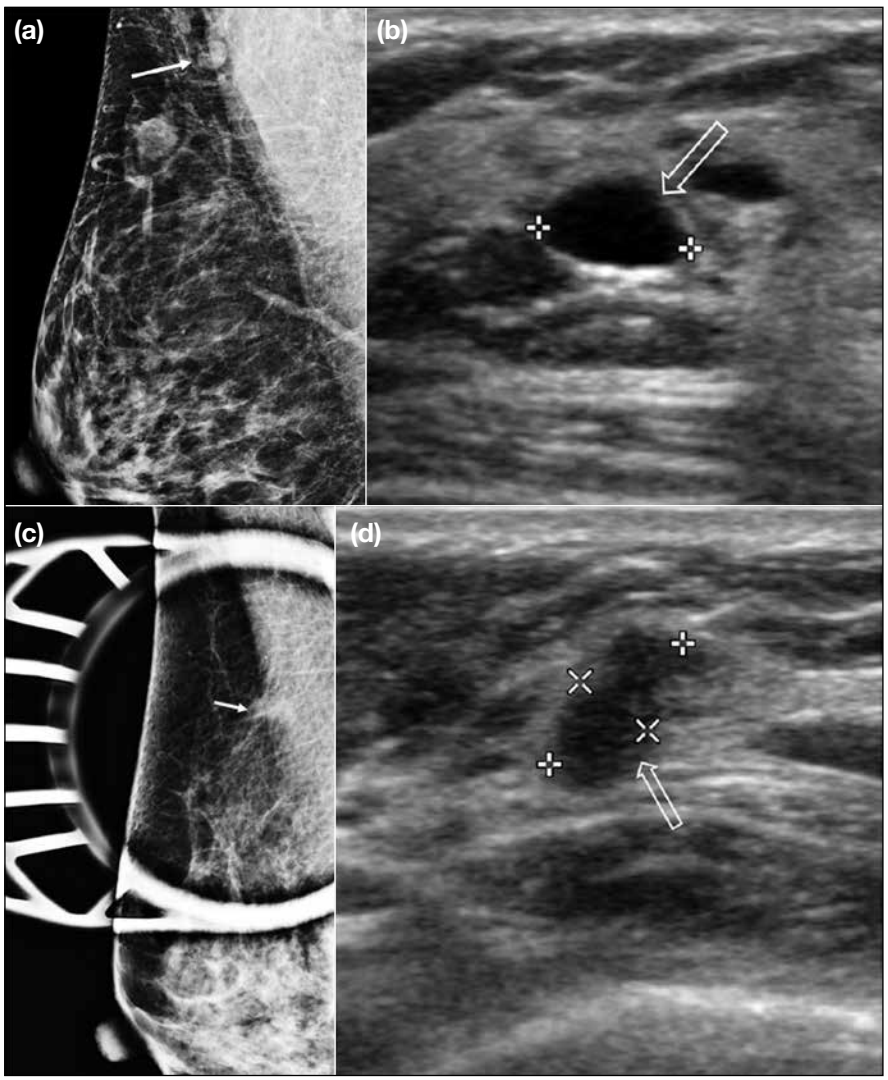

Figure 6. An axillary tail cyst that appears as (a) an oval circumscribed low-density lesion (arrow) on mammography and (b) a circumscribed cystic lesion (open arrow) on ultrasonography. (c) Spot compression mammogram of the breast showing an irregular high-density mass with spiculated margin in the axillary tail region (arrow) that was later shown to be a biopsy-proven invasive ductal carcinoma. (d) Corresponding ultrasonogram showing a non-parallel lesion with irregular margin (open arrow).

SKIN

US is the optimal imaging modality to localise superficial breast lesions.[11] Sonographic features that suggest a lesion of dermal origin include an acute angle between the lesion and the dermal line, and a "claw" of skin wrapping around the margin of a lesion.[11]

Epidermal Inclusion Cyst

Epidermal inclusion cyst (Figure 7) is a benign dermal lesion containing keratin and is lined by epidermis.[11] Its appearance on US varies with its content, ranging from cystic to hypoechoic or heterogenous.[11] The presence of a tract to the skin, which represents the hair follicle extending from the dermis up through the epidermis, is diagnostic.[11]

Pilomatricoma

Pilomatricoma is more common in children but occasionally encountered in adults.[12] It arises from the lower dermis and extends into the subcutaneous fat as it grows, with thinning of the overlying dermis.[12] On US (Figure 8), it appears as a well-defined hypoechoic mass with echogenic calcific foci, or a completely calcified mass showing strong posterior acoustic shadow.[12]

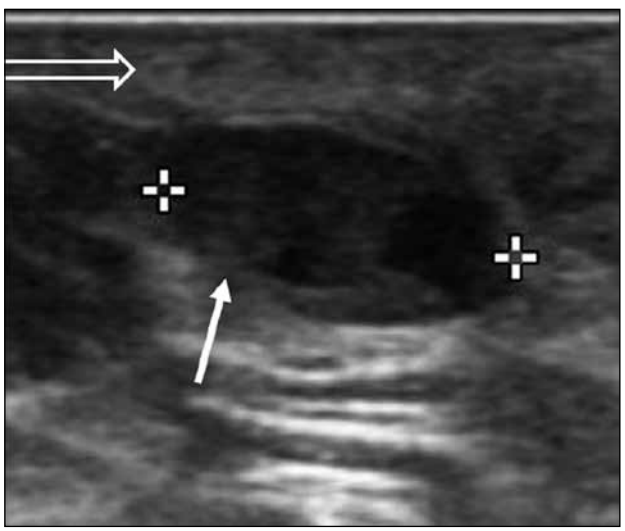

Figure 7. Ultrasonogram showing an epidermal inclusion cyst (arrow) that appears as an oval hypoechoic lesion with internal debris and contiguous with the skin (open arrow).

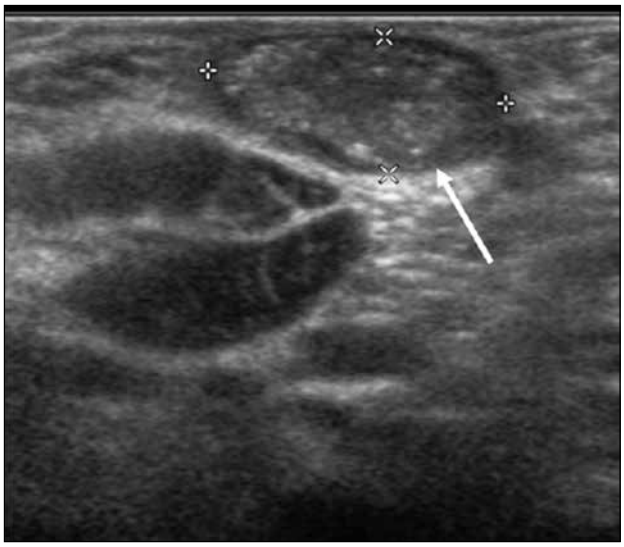

Figure 8. A pilomatricoma that appears on ultrasonography as an oval heterogeneous mass with internal calcifications (arrow) at the junction of the skin and subcutaneous fat in a child.

SUBCUTANEOUS TISSUES AND MUSCLES

Lipoma

Lipomas often have a homogeneous circumscribed appearance, some of which may have septations.[2] They are usually subcutaneous in origin (Figure 9a) but can also arise intramuscularly, including from the pectoralis muscle in the axilla (Figure 9b), manifesting as a low-density area on mammography (Figure 9c) and fat density on CT scans.[2] They show variable echogenicity on US and may be capsulated.[2] They typically demonstrate fat signal on MRI scans with minimal contrast enhancement.[2]

Liposarcoma

When a lipomatous lesion shows atypical features including heterogenicity and contrast enhancement on cross-sectioned imaging, a liposarcoma should be considered.[2] On US (Figure 10), a well-differentiated liposarcoma appears heterogeneous, multilobulated, and typically well-defined.[13] Sonographic identification of hyperechoic fat may be difficult and variable.[13] On CT and MRI scans, it usually presents as a predominantly lipomatous mass with non-lipomatous components, most often as thickened septa with or without nodularity.[13]

Other Soft Tissue Masses

Other soft tissue masses include other soft tissue sarcomas, nodular fasciitis, desmoid fibromatosis, and benign muscular neoplasms such as intramuscular myxoma.[1,4] In our centre, we came across undifferentiated pleomorphic sarcoma (Figure 11a,b) and rhabdomyosarcoma (Figure 11c) involving the axilla.

BLOOD VESSELS

Vascular Lesions

Among this heterogeneous group of axillary lesions,

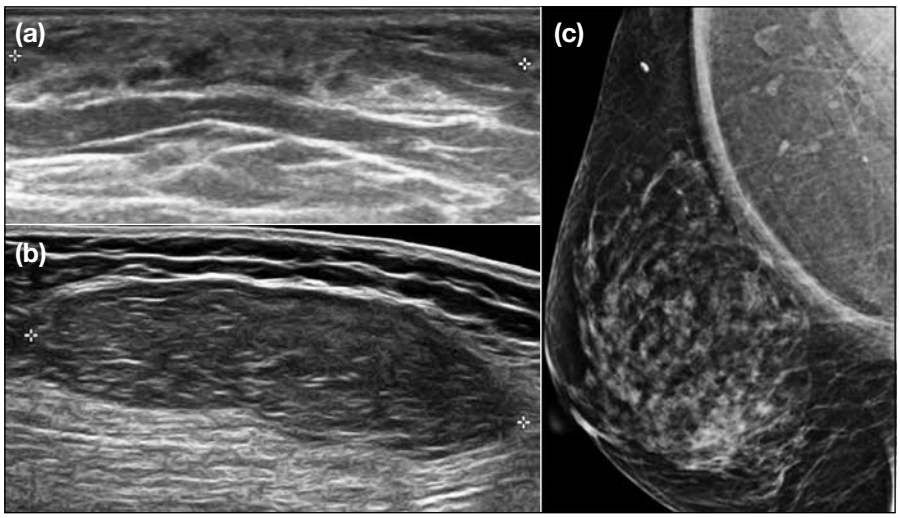

Figure 9. Ultrasonograms showing (a) a subcutaneous lipoma with echogenicity similar to adjacent subcutaneous fat and (b) an intramuscular lipoma within the pectoralis major with a capsule, and internal echogenic fibrous septa. (c) Mammogram showing an intramuscular lipoma appearing as a large low-density mass in the intrapectoral region.

Figure 10. Colour Doppler ultrasonogram showing an irregular subcutaneous mass with internal vascularity (arrow) and suspected invasion of the underlying muscle layer (open arrow), subsequently proven on histopathology to be a liposarcoma.

vascular malformation and pseudoaneurysms have been reported.[2,8]

In our centre, we encountered a case of arteriovenous malformation that manifested as a cluster of enhancing tortuous lesions on CT scans and angiography (Figure 12a,b). On MRI scans (Figure 12c,d), signal voids within the lesions on T2-weighted images indicated a high-flow component.

Pseudoaneurysms can be spontaneous or trauma-related.[14] We encountered a case of axillary artery pseudoaneurysm secondary to adjacent proximal humeral fracture. On Doppler US, typical findings include the "yin-yang" sign (Figure 13a) and a "to-and-fro" waveform on duplex Doppler US (Figure 13b), both of which are related to turbulent blood flow in the lesion.[14] Different types of angiography (conventional or CT) may also help, especially in identifying the donor artery. Pseudoaneurysm can appear as a low-density lesion on CT with enhancement similar to the donor artery while a non-enhanced region within the lesion may signify thrombosis (Figure 13c).[14]

NERVES

Peripheral nerve sheath tumours are divided into two benign entities, neurofibroma and schwannoma, and a malignant form, malignant peripheral nerve sheath tumour.[15] MRI plays an important role in the identification and characterisation of these tumours. They commonly appear as fusiform lesions and demonstrate low to intermediate signal intensity on T1-weighted sequence and high signal intensity on T2-weighted sequence.[15] Some other suggestive imaging features include the "entering or exiting nerve sign", the "split-fat" sign, the "target sign" (Figure 14a), the "fascicular sign" (Figure 14b), and atrophy of the muscles supplied by the involved nerve.[15]

BONES

Tumours arising from bones such as the proximal humerus, scapula or ribs, either primary or secondary, aggressive or non-aggressive, can present as focal swelling or mass in the axilla due to indentation or local invasion. Examples include benign osteochondroma (Figure 15a,b) and primary bone malignancy such as

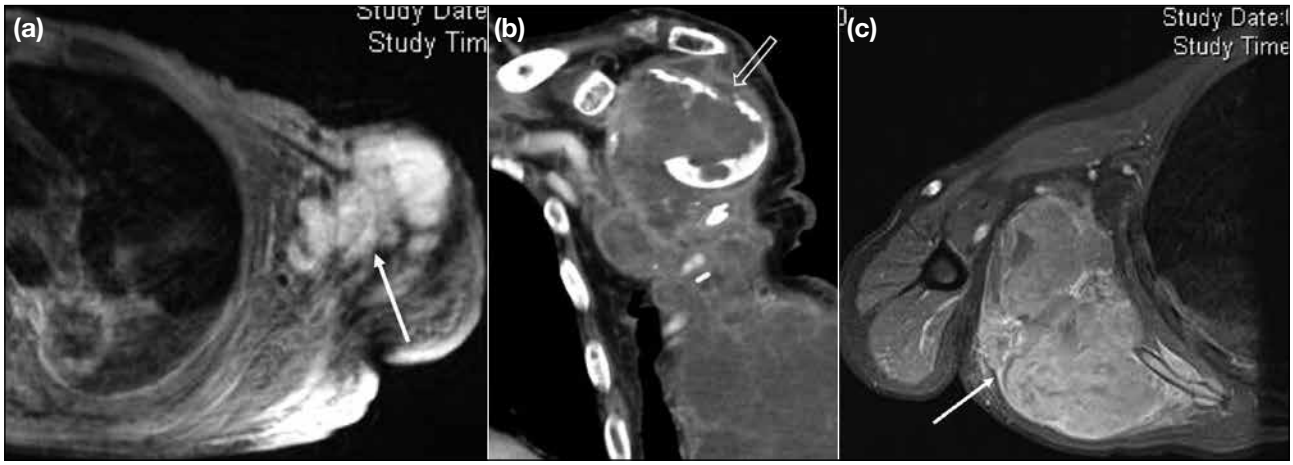

Figure 11. (a) T2-weighted magnetic resonance image showing a lobulated hyperintense mass (arrow) involving the left axilla, left chest wall, and left upper limb, involving the skin, subcutaneous, and muscle layers, subsequently proven on biopsy to be undifferentiated pleomorphic sarcoma. (b) Computed tomography scan showing a heterogeneously enhancing mass in the corresponding region with destruction of the left proximal humerus (open arrow). (c) Post-contrast T1-weighted magnetic resonance image showing a lobulated mass in the right axilla with heterogeneous enhancement involving the scapula (arrow), subsequently proven on biopsy to be rhabdomyosarcoma.

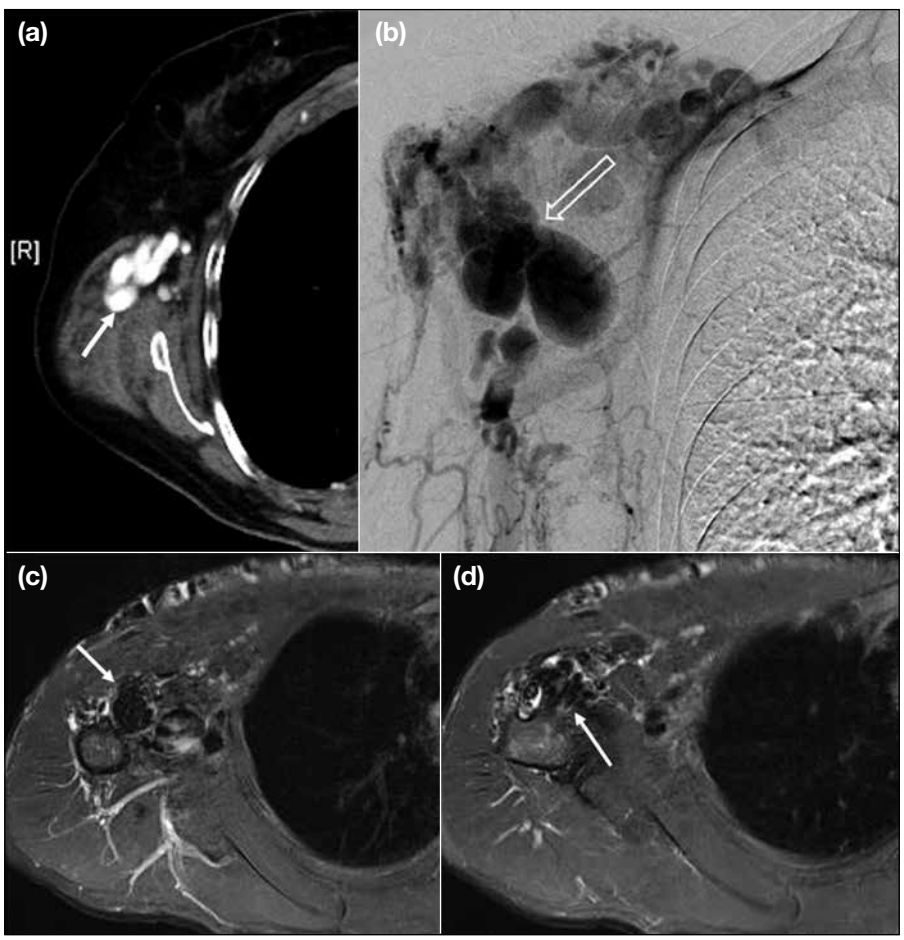

Figure 12. (a) Computed tomography scan of a cluster of serpiginous lesions (arrow) with avid enhancement in the right axilla. (b) Angiogram showing this to be a vascular malformation involving the right axillary artery (open arrow). (c, d) T2-weighted magnetic resonance images showing multiple flow-related signal voids (arrows) in the vascular malformation, consistent with a high-flow lesion.

osteogenic sarcoma. Metastasis should be considered especially in patients with a known history of primary malignancy elsewhere (Figure 15c,d).

CONCLUSION

Axillary lesions can be categorised as nodal or non-nodal lesions. A relevant clinical history including any

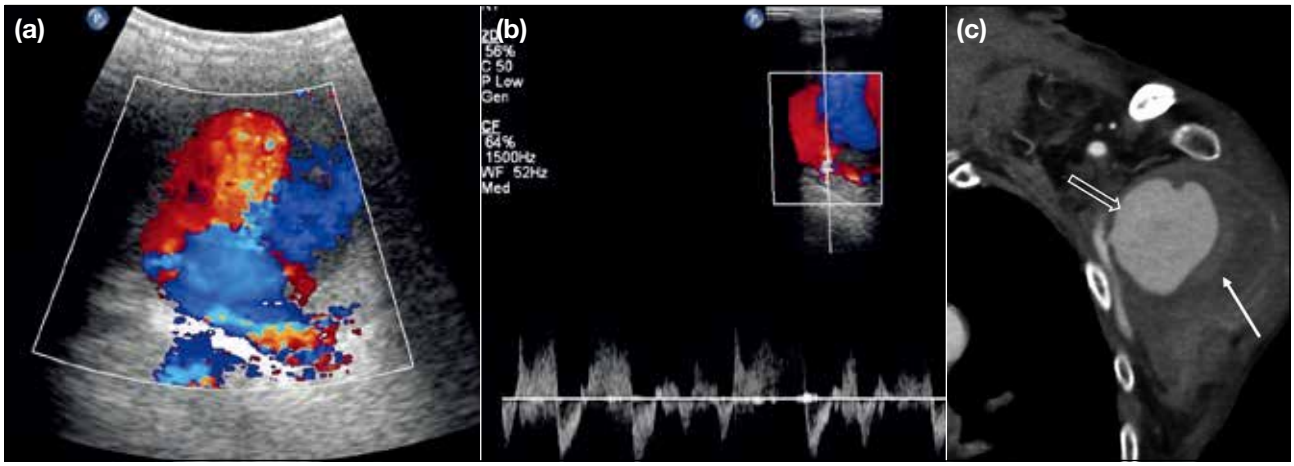

Figure 13. (a) Colour Doppler ultrasonogram of an axillary artery pseudoaneurysm demonstrates the "yin-yang" swirl pattern caused by turbulent internal flow. (b) Spectral Doppler image demonstrates a "to-and-fro" waveform, indicating a bidirectional blood flow within the pseudoaneurysm. (c) Computed tomography angiogram showing a pseudoaneurysm arising from the left axillary artery with thrombosed (arrow) and non-thrombosed (open arrow) areas.

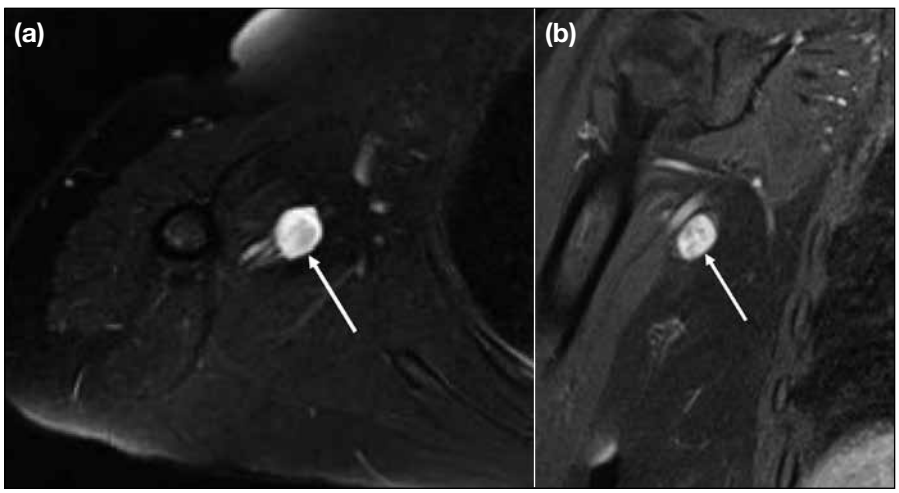

Figure 14. (a) T2-weighted magnetic resonance image showing a schwannoma (arrow) arising from the axillary nerve with the "target sign" of high signal intensity peripherally and low signal intensity centrally. The nerve roots are seen entering or exiting the lesion. (b) T1-weighted post-contrast magnetic resonance image showing fascicular sign with hypointense fascicular bundles inside a schwannoma (arrow).

known systemic diseases, infection, previous breast augmentation or recent vaccination may indicate the underlying causes of axillary lymphadenopathy. Familiarity with characteristic imaging findings such as "snowstorm sign" for nodal silicone deposits, is also useful. Lymph nodes with suspicious features warrant follow-up or tissue diagnosis. For non-nodal lesions, one should enquire if the patient has had any breast or axillary intervention or active local infection. If such a history is absent, the differential diagnoses can be narrowed down according to the anatomical origin of the lesion.

REFERENCES

1. Oliff MC, Birdwell RL, Raza S, Giess CS. The breast imager's approach to nonmammary masses at breast and axillary US: imaging technique, clues to origin, and management. Radiographics. 2016;36:7-18.
2. Gupta A, Metcalf C, Taylor D. Review of axillary lesions, emphasising some distinctive imaging and pathology findings. J Med Imaging Radiat Oncol. 2017;61:571-81.
3. Dialani V, James DF, Slanetz PJ. A practical approach to imaging the axilla. Insights Imaging. 2015;6:217-29.
4. Pinheiro DJ, Elias S, Nazário AC. Axillary lymph nodes in breast cancer patients: sonographic evaluation. Radiol Bras. 2014;47:240-4.
5. Mendelson EB, Böhm-Vélez M, Berg WA, Whitman GJ, Feldman MI, Madjar H, et al. ACR BI-RADS ultrasound. In: D'Orsi CJ, Sickles EA, Mendelson EB, Morris EA, editors. ACR BI-RADS Atlas: Breast Imaging Reporting and Data System. Reston: American College of Radiology; 2013.
6. Ikeda DM, Miyake KK. Breast Imaging: The Requisites. 3rd ed. Elsevier; 2017. p 422-5.
7. Mehta N, Sales RM, Babagbemi K, Levy AD, McGrath AL,

Figure 15. (a) Plain radiograph showing lytic metastasis in the left scapula (arrow) with soft tissue swelling extending to the left axilla in a patient with known renal cell carcinoma. (b) Computed tomography image confirms the presence of a heterogeneously enhancing mass consistent with metastasis (open arrow). (c) T1-weighted and (d) T2-weighted magnetic resonance images showing an osteochondroma arising from the medial aspect of the proximal left humerus with T1 hypointense, T2 hyperintense cartilaginous cap (arrows). No abnormal signal is present in the surrounding soft tissues or underlying marrow.

Drotman M, et al. Unilateral axillary adenopathy in the setting of COVID-19 vaccine. Clin Imaging. 2021;75:12-5.
8. Park YM, Park JS, Yoon HK, Yang WT. Imaging-pathologic correlation of diseases in the axilla. AJR Am J Roentgenol. 2013;200:W130-42.
9. Wong T, Lo LW, Fung PY, Lai HY, She HL, Ng WK, et al. Magnetic resonance imaging of breast augmentation: a pictorial review. Insights Imaging. 2016;7:399-410.
10. Okubo M, Tada K, Niwa T, Nishioka K, Tsuji E, Ogawa T, et al. A case of breast cancer in the axillary tail of Spence — enhanced magnetic resonance imaging and positron emission tomography for diagnostic differentiation and preoperative treatment decision. World J Surg Oncol. 2013;11:217.
11. Giess CS, Raza S, Birdwell RL. Distinguishing breast skin lesions from superficial breast parenchymal lesions: diagnostic criteria, imaging characteristics, and pitfalls. Radiographics. 2011;31:1959-72.
12. Hwang JY, Lee SW, Lee SM. The common ultrasonographic features of pilomatricoma. J Ultrasound Med. 2005;24:1397-402.
13. Murphey MD, Arcara LK, Fanburg-Smith J. From the archives of the AFIP: imaging of musculoskeletal liposarcoma with radiologic-pathologic correlation. Radiographics. 2005;25:1371-95.
14. Saad NE, Saad WE, Davies MG, Waldman DL, Fultz PJ, Rubens DJ. Pseudoaneurysms and the role of minimally invasive techniques in their management. Radiographics. 2005;25 Suppl 1:S173-89.
15. Chee DW, Peh WC, Shek TW. Pictorial essay: imaging of peripheral nerve sheath tumours. Can Assoc Radiol J. 2011;62:176-82.